# Ruxolitinib reverses dysregulated T helper cell responses and controls autoimmunity caused by a novel signal transducer and activator of transcription 1 (STAT1) gain-of-function mutation

Katja G. Weinacht, MD, PhD,[a,b]*‡ Louis-Marie Charbonnier, PhD,[c]* Fayhan Alroqi, MD,[c] Ashley Plant, MD,[a,b] Qi Qiao, PhD,[d] Hao Wu, PhD,[c,d] Clement Ma, PhD,[a,b] Troy R. Torgerson, MD, PhD,[e,f] Sergio D. Rosenzweig, MD, PhD,[g,h] Thomas A. Fleisher, MD,[h] Luigi D. Notarangelo, MD,[c,i] Imelda C. Hanson, MD,[j] Lisa R. Forbes, MD,[j] and Talal A. Chatila, MD, MSc[c]   *Boston and Cambridge, Mass, Seattle, Wash, Bethesda, Md, and Houston, Tex*

GRAPHICAL ABSTRACT
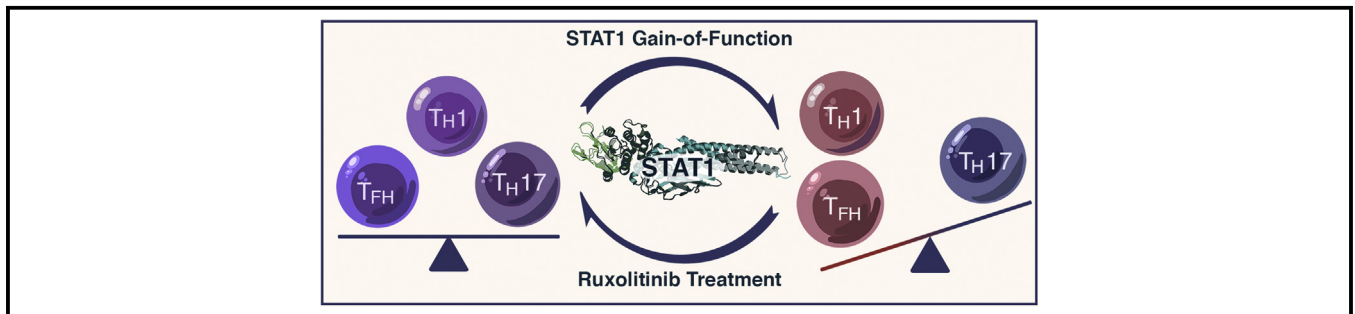
Background: Gain-of-function (GOF) mutations in the human signal transducer and activator of transcription 1 (STAT1) manifest in immunodeficiency and autoimmunity with impaired T_H17 cell differentiation and exaggerated responsiveness to type I and II interferons. Allogeneic bone marrow transplantation has been attempted in severely affected patients, but outcomes have been poor.

Objective: We sought to define the effect of increased STAT1 activity on T helper cell polarization and to investigate the therapeutic potential of ruxolitinib in treating autoimmunity secondary to STAT1 GOF mutations.

Methods: We used *in vitro* polarization assays, as well as phenotypic and functional analysis of STAT1-mutated patient cells.

Results: We report a child with a novel mutation in the linker domain of STAT1 who had life-threatening autoimmune cytopenias and chronic mucocutaneous candidiasis. Naive lymphocytes from the affected patient displayed increased T_H1 and follicular T helper cell and suppressed T_H17 cell responses. The mutation augmented cytokine-induced STAT1 phosphorylation without affecting dephosphorylation kinetics. Treatment with the Janus kinase 1/2 inhibitor

ruxolitinib reduced hyperresponsiveness to type I and II interferons, normalized T_H1 and follicular T helper cell responses, improved T_H17 differentiation, cured mucocutaneous candidiasis, and maintained remission of immune-mediated cytopenias.

Conclusions: Autoimmunity and infection caused by *STAT1* GOF mutations are the result of dysregulated T helper cell responses. Janus kinase inhibitor therapy could represent an effective targeted treatment for long-term disease control in severely affected patients for whom hematopoietic stem cell transplantation is not available. (J Allergy Clin Immunol 2017;■■■:■■■-■■■.)

Key words: STAT1 *gain of function, IFN-γ, ruxolitinib, autoimmunity,* T_H1 *cell,* T_H17 *cell, follicular T helper cell, T helper cell polarization*

Signal transducer and activator of transcription 1 (STAT1) is a member of the STAT family of transcription factors which play a key role in the cellular response to interferons and is a central component in many other signaling pathways, including interleukins, growth factors, and hormones. In response to extracellular receptor stimulation, Janus kinase (JAK) activation leads to phosphorylation of cytoplasmic STAT1, followed by homodimerization or heterodimerization with other phosphorylated STAT family members. The dimers translocate into the nucleus and bind designated promoter elements to activate transcription of their respective target genes.[1-3]

STAT1 is the target of both loss-of-function and gain-of-function (GOF) mutations. Whereas the former are associated with susceptibility to mycobacterial and/or viral infections, the latter give rise to a mixed phenotype of autoimmunity, mucocutaneous candidiasis, and invasive fungal infections related to augmented T_H1 and diminished T_H17 cell responses.[4-9] *STAT1* GOF mutations prompt a signal-induced increase in levels of phosphorylated STAT1 (phospho-STAT) and amplified transcription of interferon-responsive genes, which lead to autoimmunity.[5,6,10] Delayed dephosphorylation with ensuing accumulation of phospho-STAT1 in the nucleus has been proposed as a mechanistic basis in most reported cases.[1,6,11-15] How increased STAT1 activity compromises T_H17 immunity to result in chronic mucocutaneous candidiasis and other invasive fungal and viral infections is less well understood.[12,16,17] Excessive production of interferons, IL-27, and programmed death (PD) 1 ligand can directly impair T_H17 cell differentiation.[18,19] Alternatively, predominance of STAT1 signaling over STAT3 signaling might deviate the response to IL-6, IL-21, and IL-23 away from STAT3, which normally mediates T_H17 cell development.[1,18]

The clinical management of patients with *STAT1* GOF mutations remains challenging.[20-22] In particular, controlling autoimmunity is difficult because conventional immunosuppression adds to the already increased risk of infections. Therapy-refractory or life-threatening disease is considered a noncanonical indication for allogeneic hematopoietic stem cell transplantation; however, the immune phenotype of *STAT1* GOF mutations amplifies the transplant-related risk for uncontrolled infections and graft-versus-host disease, contributing further to the poor prognosis.[21,23]

Liu et al[24] were the first to provide proof of principle that JAK inhibitors can successfully treat STAT1-mediated hyperresponsiveness to interferons in patients with vascular and pulmonary syndrome caused by mutations in *TMEM173*, which encodes the stimulator of interferon genes. Higgins et al[10] reported hair regrowth in a patient with alopecia areata secondary to a *STAT1* GOF mutation after treatment with ruxolitinib. Most recently, Mössner et al[25] observed improvement of chronic mucocutaneous candidiasis with ruxolitinib and a reactive increase in IL-17A/F levels.

Here we describe the immunophenotypic analysis of a patient with life-threatening autoimmune cytopenias and a novel GOF mutation in the linker domain of *STAT1*. Importantly, in addition to increasing T_H1 and suppressing T_H17 cell differentiation, the augmented STAT1 activity dysregulated follicular T helper (T_{FH}) cell responses. This finding was corroborated in a different patient with known $STAT1^{T385M}$ GOF mutation in the DNA-binding domain who presented solely with chronic mucocutaneous candidiasis and opportunistic infections but without clinical evidence of autoimmunity.[13,26,27] Long-term treatment with the JAK inhibitor ruxolitinib decreased the increased STAT1 phosphorylation, reversed the dysregulated T_H1 and T_{FH} cell development, improved the previously impaired T_H17 response, and enabled effective control of the autoimmune cytopenias. This is the first report demonstrating mechanistic evidence that pharmacologic manipulation of the JAK-STAT pathway in patients with *STAT1* GOF mutations leads to reversal of the immune dysregulation phenotype and provides proof of principle that JAK inhibitors are not only effective in treating active autoimmune disease and immunodeficiency secondary to hyperresponsiveness of STAT1 but also in reversing the aberrant priming of naive cells, thereby maintaining long-term disease control and sustained remission.

METHODS
Patients and healthy subjects
All study participants were recruited after obtaining written informed consent approved by the Boston Children's Hospital Institutional Review Board.

Pharmacotherapy
The IL-1 receptor antagonist anakinra (Kineret; Sobi, Stockholm, Sweden) was administered intravenously twice daily at a dose of 100 mg.

Four infusions with equine anti-thymocyte globulin (ATG; Atgam; Pfizer, New York, NY) were administered intravenously at a dose of 40 mg/kg body weight per infusion 24 hours apart. Supportive therapy during the infusions consisted of acetaminophen, diphenhydramine, and methylprednisolone.

Treatment with intravenous cyclosporine (SandIMMUNE; Novartis, East Hanover, NJ) was initiated on day 1 of ATG therapy at a dose of 4 mg/kg body

weight per day and titrated to a serum level of 175 to 250 μg/L. The route of administration was converted to oral after 4 weeks, maintaining the same serum target level.

Eculizumab (Soliris; Alexion Pharmaceuticals, Cheshire, Conn) was administered intravenously at a dose of 600 mg per infusion. Only 1 infusion was administered because of a lack of efficacy. Supportive therapy during the infusion consisted of acetaminophen, diphenhydramine, and methylprednisolone. The patient received a meningococcal vaccination prior to treatment with eculizumab, as well as meningococcal prophylaxis with azithromycin for 6 months after infusion.

Rituximab (Rituxan; Genentech, South San Francisco, Calif) was administered intravenously at a dose of 375 mg/m^2 body surface area (BSA) once weekly for 4 consecutive weeks. Supportive therapy during the infusions consisted of acetaminophen, diphenhydramine, and methylprednisolone.

Treatment with ruxolitinib (Jakafi; Incyte, Wilmington, Del) was initiated at a low dose of 5 mg/m^2 BSA once daily because of concomitant use of other CYP3A4-inhibiting medications. The ruxolitinib dose was escalated until the amount of phospo-STAT1 induced in the patient's CD4$^+$ T cells was equal to that in healthy control cells. The final therapeutic ruxolitinib dose was 10 mg/m^2 BSA per day administered orally in 2 divided doses.

STAT1 sequencing

Exons 3 to 23 of STAT1, including exon/intron boundaries, were amplified from genomic DNA by means of PCR and sequenced bidirectionally with dye-terminator chemistry. PCR amplification of exon 20 was carried out with the following primers: STAT1E20_F (GATAAGAGCGGGGAGGG) and STAT1E20_R (TGAAGCTGGACTCAGGC). The mutation was predicted to be deleterious by using SIFT and PolyPhen-2.[28,29]

Protein modeling

The STAT1^{E545K} mutant structure was generated by using SWISS-MODEL with STAT1 structures (PDB code: 1YVL and 1BF5).[30-33] Structural alignment was performed in Coot, and molecular representation was displayed in PyMOL.[34]

Antibodies and flow cytometry

Monoclonal antibodies to the following human proteins were used for staining: CD3 (UCHT1), CD4 (RPA-T4), CD8 (RPA-T8), CD45RA (HI100), CCR7 (G043H7), inducible costimulator (ICOS; C398.4A), PD1 (eBioJ105), CXCR5 (MU5UBEE), phospho-STAT1 (KIKSI0803), and phospho-STAT3 (LUVNKLA; all from eBioscience, San Diego, Calif); IL-17 (BL168), IFN-γ (4S.B3), CCR6 (G034E3), and CXCR3 (G025H7; all from BioLegend, San Diego, Calif); and STAT1 (246523; R&D Systems, Minneapolis, Minn). Appropriate isotype controls were used in parallel. PBMCs were incubated with mAbs against surface proteins for 30 minutes on ice.

Intracellular STAT1 staining

STAT1 staining was performed with an eBioscience Fixation/Permeabilization kit, according to the manufacturer's instructions.

Phospho-STAT1 and phospho-STAT3 staining

PBMCs were stimulated in complete medium for 20 minutes with appropriate cytokines: human IFN-β (20 ng/mL; Miltenyi Biotec, Bergisch Gladbach, Germany), IFN-γ, or IL-21 (20 ng/mL; PeproTech, Rocky Hills, NJ). Subsequently, PBMCs were fixed with 2% paraformaldehyde for 20 minutes on ice, permeabilized with 90% methanol for 30 minutes on ice, and stained with CD3, CD4, phospho-STAT1, and phospho-STAT3 mAbs in PBS for 30 minutes.

Ex vivo cytokine detection

PBMCs were isolated from whole blood by means of centrifugation over a Ficoll gradient and stimulated in complete medium in the presence of anti-CD2/CD3/CD28 beads (Miltenyi Biotec) and 100 U/mL recombinant human IL-2 (PeproTech) for 2 days. Subsequently, cell suspensions were incubated with phorbol 12-myristate 13-acetate (50 ng/mL; Sigma-Aldrich, St Louis, Mo), ionomycin (500 ng/mL; Sigma-Aldrich), and GolgiPlug (BD Biosciences, San Jose, Calif), according to the manufacturer's instructions, in complete medium for 4 hours before surface staining. Permeabilization and intracellular IFN-γ and IL-17 staining were carried out with an eBioscience Fixation/Permeabilization kit, as described above. Data were collected with an LSRFortessa cytometer (BD Biosciences) and analyzed with FlowJo software (TreeStar, Ashland, Ore).

JAK inhibitor treatment *in vitro*

PBMCs were incubated for 4 hours in the presence of different concentrations of ruxolitinib, which is primarily a JAK1/2 inhibitor (10 or 100 nmol/L; Selleckchem, Houston, Tex), and tofacitinib, which is predominantly a JAK3 inhibitor (10 and 100 nmol/L; Sigma-Aldrich), or vehicle (dimethyl sulfoxide) alone before stimulation with recombinant human IFN-β (20 ng/mL; Miltenyi Biotec), IFN-γ, or IL-21 (20 ng/mL, PeproTech).

T helper cell subset differentiation

CD4$^+$ T cells were enriched from PBMCs by means of negative selection with magnetic beads (Miltenyi Biotec), and naive CD45RA$^+$CCR7$^+$CD4$^+$ T cells were then isolated by means of cell sorting with a BD FACSAria cytometer. Naive CD4$^+$ T cells were seeded at a concentration of 5×10^5 cells per well in a 96-well plate in complete medium and stimulated with anti-CD2/CD3/CD28 beads (Miltenyi Biotec) alone (T$_H$0 condition) or in the presence of recombinant human cytokines: IL-12 (20 ng/mL) for T$_H$1 conditions (BioLegend); IL-6 (20 ng/mL), IL-23 (10 ng/mL; both from BioLegend), and TGF-β1 (5 ng/mL; R&D Systems) for T$_H$17 conditions; and IL-12 (2 ng/mL), IL-23 (10 ng/mL), and TGF-β1 (5 ng/mL) for T$_{FH}$ conditions.[35]

Statistical analysis

Comparisons between the patient and healthy control subjects were analyzed by using the unpaired Student *t* test and 1- or 2-way ANOVA with posttest analysis. Two-sided *P* values of less than .05 were considered statistically significant.

RESULTS

Refractory autoimmune cytopenias associated with a novel STAT1 GOF mutation

A 10-year-old girl with a longstanding history of Evans syndrome manifesting in autoimmune hemolytic anemia and immune thrombocytopenia presented to our institution with an acute exacerbation of her disease (in the following referred to as "the" patient or patient 1). She required daily packed red blood cell transfusions to keep her hemoglobin level at greater than 6 g/dL and experienced systemic bleeding symptoms refractory to platelet transfusion. At presentation, the patient had already been treated with a prolonged course of steroids and multiple doses of intravenous immunoglobulins. Although these therapies did not induce remission, withdrawal of steroids spurred the rate of hemolysis further, necessitating continued glucocorticoid therapy.

The patient had a history of chronic mucocutaneous candidiasis involving her nails, oral mucosa, and vaginal tract. She also had chronic diarrhea and severe chronic lung disease with respiratory insufficiency requiring supplemental oxygen. She was a poor responder to vaccines and had been treated with immunoglobulin replacement over extended periods of her life. The parents were nonconsanguineous, and there was no family history of
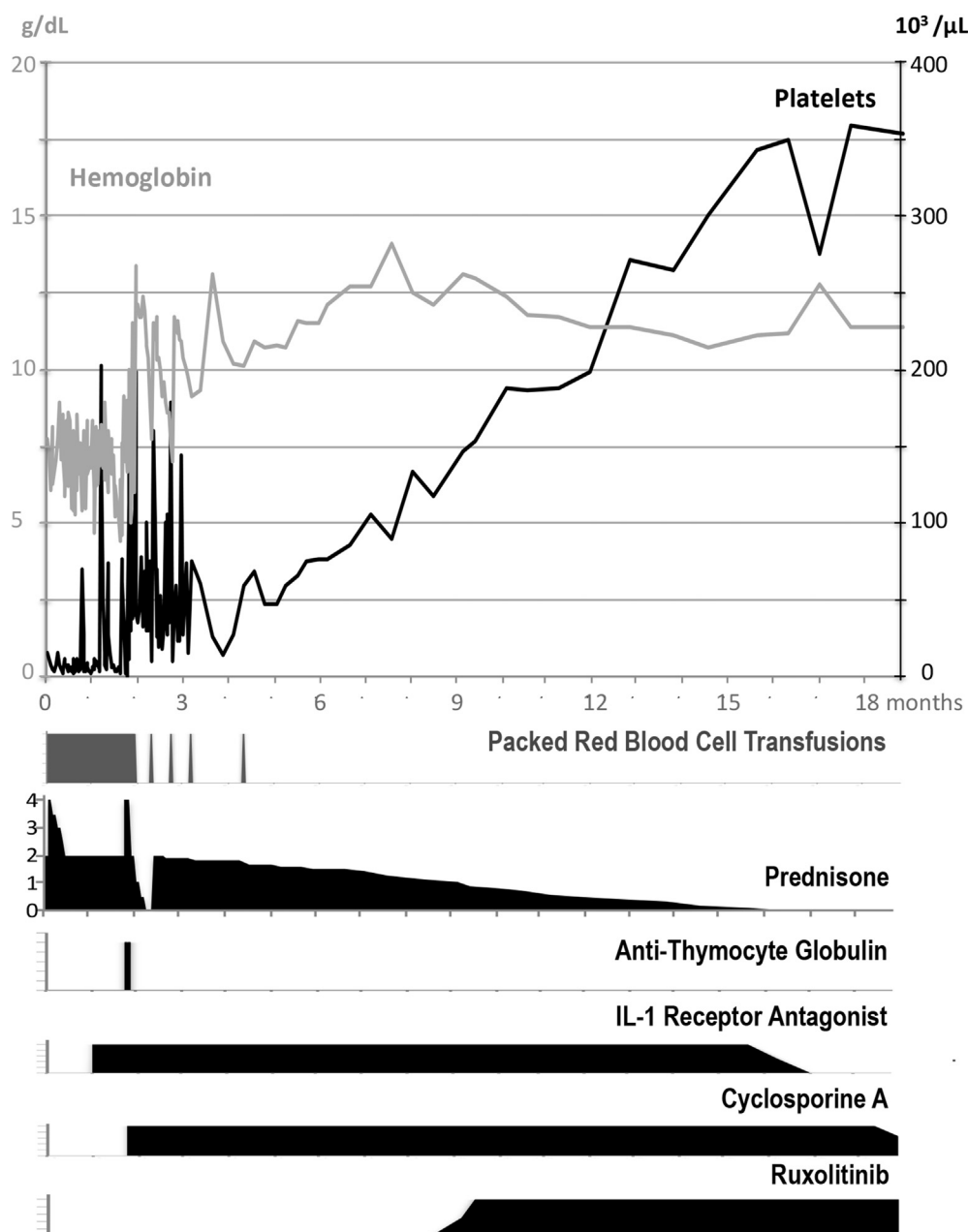
FIG 1. Hemoglobin and platelet count in response to pharmacotherapy. The graph depicts serum hemoglobin concentration in grams per deciliter *(gray curve)* and platelet count in 10^3 cells per microliter *(black curve)* in response to changes in steroid dose, as well as pharmacotherapy with ATG, the IL-1 receptor antagonist anakinra, cyclosporine, and ruxolitinib. Timing of packed red blood cell transfusions is indicated in dark gray. The prednisone dose is expressed in milligrams per kilogram body weight.

autoimmunity, immunodeficiency, or other blood dyscrasias. HLA typing revealed that the patient's only sibling was not a match.

A comprehensive diagnostic evaluation revealed positive antiplatelet IgM antibody levels, as well as a complement-fixing, high-affinity, high-thermal-amplitude cold agglutinin. Consequently, the patient received a course of the anti-CD20 mAb rituximab followed by the anti-complement C5 antibody eculizumab without clinical improvement. Over the course of the following 6 weeks, the patient's reticulocyte count and absolute neutrophil count started to decrease, whereas ferritin and lactate dehydrogenase levels were increasing. Serial bone marrow biopsies demonstrated a steady decrease in bone marrow cellularity from greater than 70% before admission to less than 10% 11 weeks later, leading to the diagnosis of acquired aplastic anemia. A bone marrow aspirate also revealed occasional $CD163^+$ hemophagocytic histiocytes, for which treatment with the IL-1 receptor antagonist anakinra for presumed macrophage activation syndrome was added to the baseline steroid therapy.

A diagnostic workup for genetic causes of bone marrow failure was nonrevealing. Accordingly, the patient received standard immunosuppressive therapy for idiopathic aplastic anemia
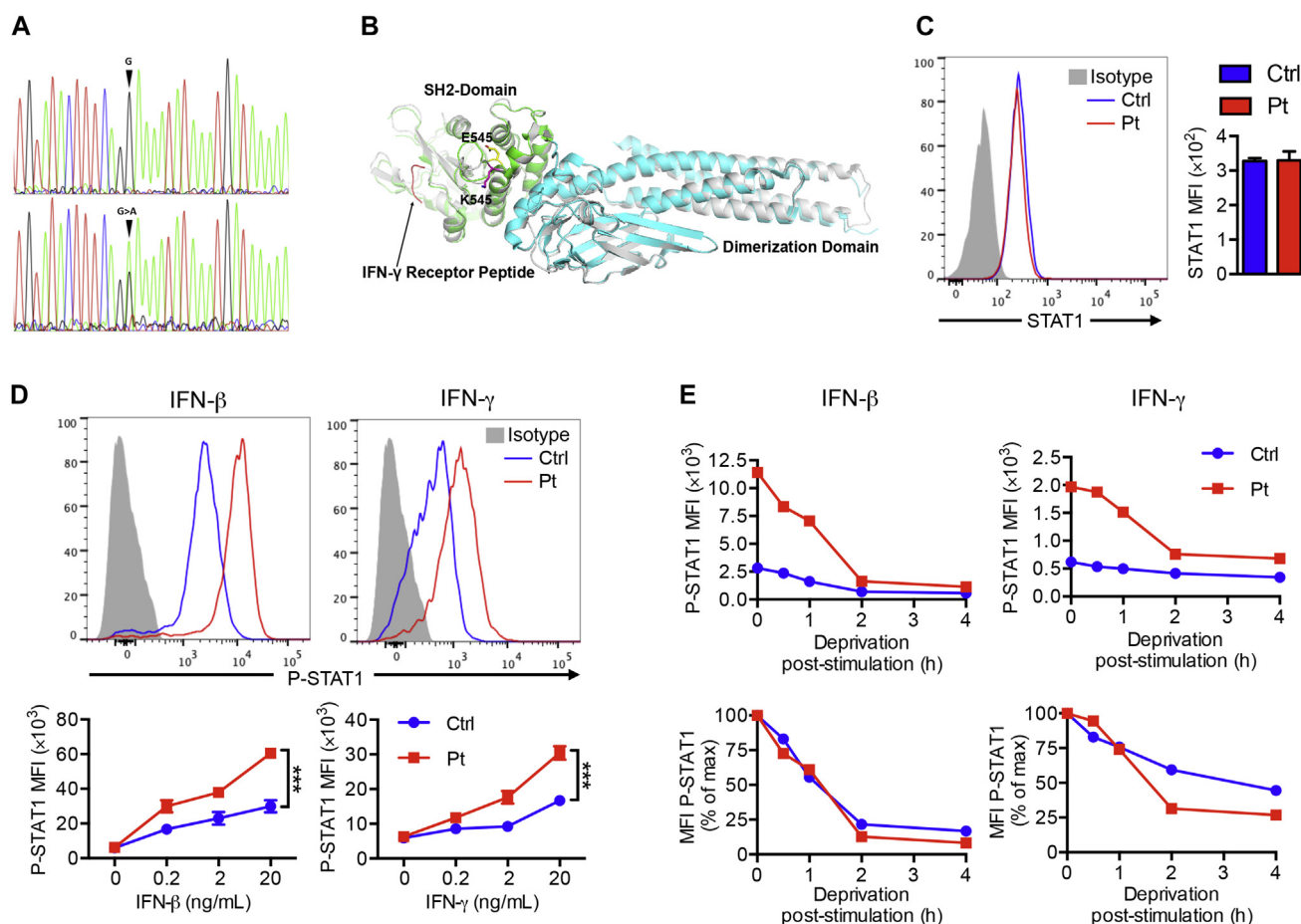
FIG 2. $STAT1^{E545K}$ mutation leads to hyperphosphorylation GOF. **A,** Sanger sequencing revealed a monoallelic c.1633G>A substitution in *STAT1*. **B,** Structural alignment between STAT1 structure and modeled E545K mutant structure (white). WT domains are colored (SH2 in green, dimerization domain in cyan, and IFN-γ peptide in orange) to highlight their position relative to residue 545 (WT structure in yellow and mutant in magenta). **C,** Total STAT1 expression in CD4$^+$ T cells determined by means of flow cytometry in patient 1 and a control subject. **D,** Phospho-STAT1 *(P-STAT1)* expression in CD4$^+$ T cells stimulated with IFN-β (20 ng/mL) and IFN-γ (20 ng/mL) in the patient and a control subject *(top)* and dose-response curve with increasing interferon concentrations *(bottom).* **E,** Dephosphorylation kinetics of phospho-STAT1 in response to deprivation of IFN-β and IFN-γ in CD4$^+$ T cells represented as absolute mean fluorescence intensity *(MFI; top)* and normalized to maximum expression before deprivation *(bottom).* ***$P < .001$, 2-way ANOVA.

without an available matched sibling donor consisting of 4 doses of equine ATG and cyclosporine. Although the initial posttreatment course was complicated by intraventricular hemorrhage and acute respiratory decompensation, over the following 8-week period, the patient's clinical course stabilized. The absolute neutrophil and reticulocyte counts began to increase, which is consistent with bone marrow recovery in response to treatment with ATG and cyclosporine. However, hemolysis started to flare, and hemoglobin levels rapidly decreased again as soon as steroids were weaned, indicating that ATG and cyclosporine successfully treated the patient's aplastic anemia but did not bring the autoimmune cytopenias into complete remission (Fig 1 and see Fig E1 in this article's Online Repository at www.jacionline. org). Together with the development of acute steroid-induced diabetes, the need for an alternate therapy to control the persisting autoimmune cytopenias became critical.

Unbiased genetic testing for 200 known/selected inborn errors of immunity identified a monoallelic *de novo* missense mutation in the coding region of *STAT1* that resulted in an amino acid substitution in the linker domain of the protein and was predicted to be deleterious by using SIFT and PolyPhen-2 (c.1633G>A; p.E545K; Fig 2, *A* and *B*). Structure modeling revealed that the E545 residue is far away from the previously proposed STAT1 dimerization interface but close to the SH2 domain, which binds the activating IFN-γ receptor peptide, suggesting that this mutation might affect STAT dimer binding to cytokine receptors or kinases.[32] This mutation did not affect expression of total STAT1 protein in CD4$^+$ and CD8$^+$ T cells or in B cells at baseline (Fig 2, *C*, and data not shown). However, on stimulation of PBMCs with IFN-β (20 ng/mL) or IFN-γ (20 ng/mL) the patient's CD4$^+$ T cells demonstrated a significant increase in STAT1 phosphorylation compared with that seen in control cells (Fig 2, *D*). Unlike other reported *STAT1* GOF mutations, the E545K mutation did not affect the dephosphorylation kinetics on cytokine deprivation, which led to normalization of phospho-STAT1 expression down to baseline levels in cells
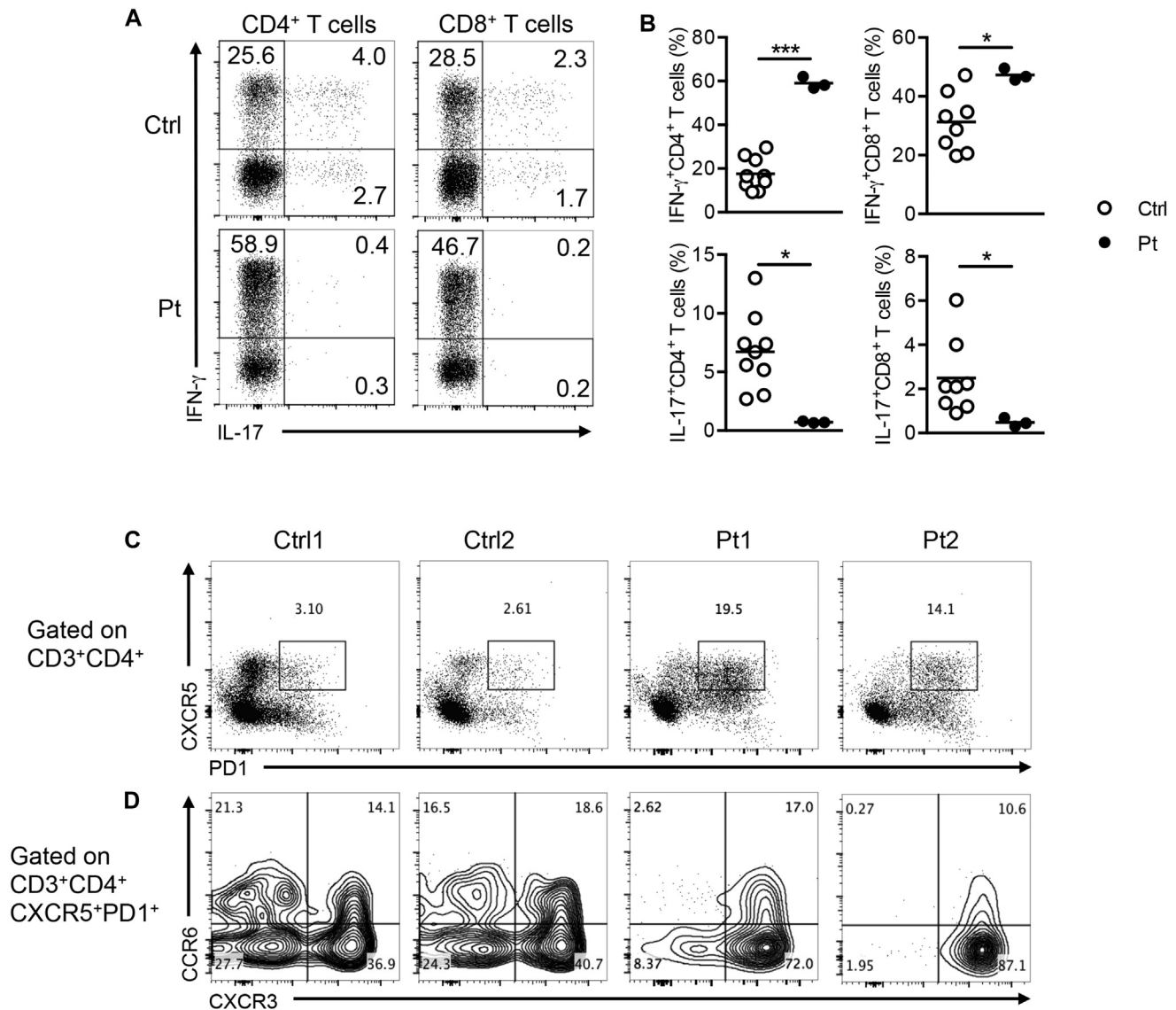
FIG 3. $STAT1^{E545K}$ GOF mutation results in exacerbated T_H1/T_C1 and T_{FH} cell responses and impaired T_H17/cytotoxic T type 17 (T_c17) immunity. **A,** Representative flow cytometric analyses of IL-17 and IFN-γ secretion by peripheral CD4$^+$ and CD8$^+$ T cells from the $STAT1^{E545K}$ patient and control subjects. **B,** Dot plots represent frequencies of IFN-γ– and IL-17–producing CD4$^+$ and CD8$^+$ T cells in each group (n = 8-9 individual control subjects and the $STAT1^{E545K}$ patient at 3 different time points). **C,** CXCR5 and PD1 expression in CD4$^+$ T cells from patient 1 $(STAT1^{E545K})$ and patient 2 $(STAT1^{T385M})$ compared with healthy control subjects. **D,** CXCR3 and CCR6 expression in CD4$^+$CXCR5$^+$PD1$^+$ T cells from patients 1 and 2 and healthy control subjects (gates shown above). *$P < .05$ and ***$P < .001$.

from the patient and control subjects over the same amount of time (Fig 2, *E*). Similar results were found on stimulation and withdrawal of the patient's CD8$^+$ T cells with the respective interferon (data not shown). These results suggest that the E545K mutation is an atypical *STAT1* GOF mutation leading to hyperphosphorylation of STAT1 in response to type I and II interferons without interfering with the dephosphorylation process.

$STAT1^{E545K}$ mediates exaggerated T_H1/cytotoxic T type 1 (T_C1) skewing and suppresses T_H17 cell differentiation

Examination of PBMCs 6 months after ATG and rituximab therapy revealed that the patient had a higher proportion of IFN-γ–producing and lower proportion of IL-17–producing circulating CD4$^+$ and CD8$^+$ T cells compared with healthy control subjects (Fig 3, *A* and *B*). To gain insight into the link between the $STAT1^{E545K}$ mutation and the patient's clinical presentation with autoimmunity, we evaluated the number of T_{FH} cells, which were defined as CD4$^+$CXCR5$^+$PD1$^+$ cells.[35,36] The patient's CD4$^+$ T cells showed an approximately 7-fold increase in the fraction of CXCR5$^+$PD1$^+$ T_{FH} cells compared with healthy control cells (Fig 3, *C*), which is suggestive of an increased risk of dysregulated humoral immunity conferred by the $STAT1^{E545K}$ mutation.

To corroborate the hypothesis that dysregulated T_{FH} cell immunity is a primary feature of amplified STAT1 activity, we selected a second patient (patient 2) with a different $STAT1^{T385M}$
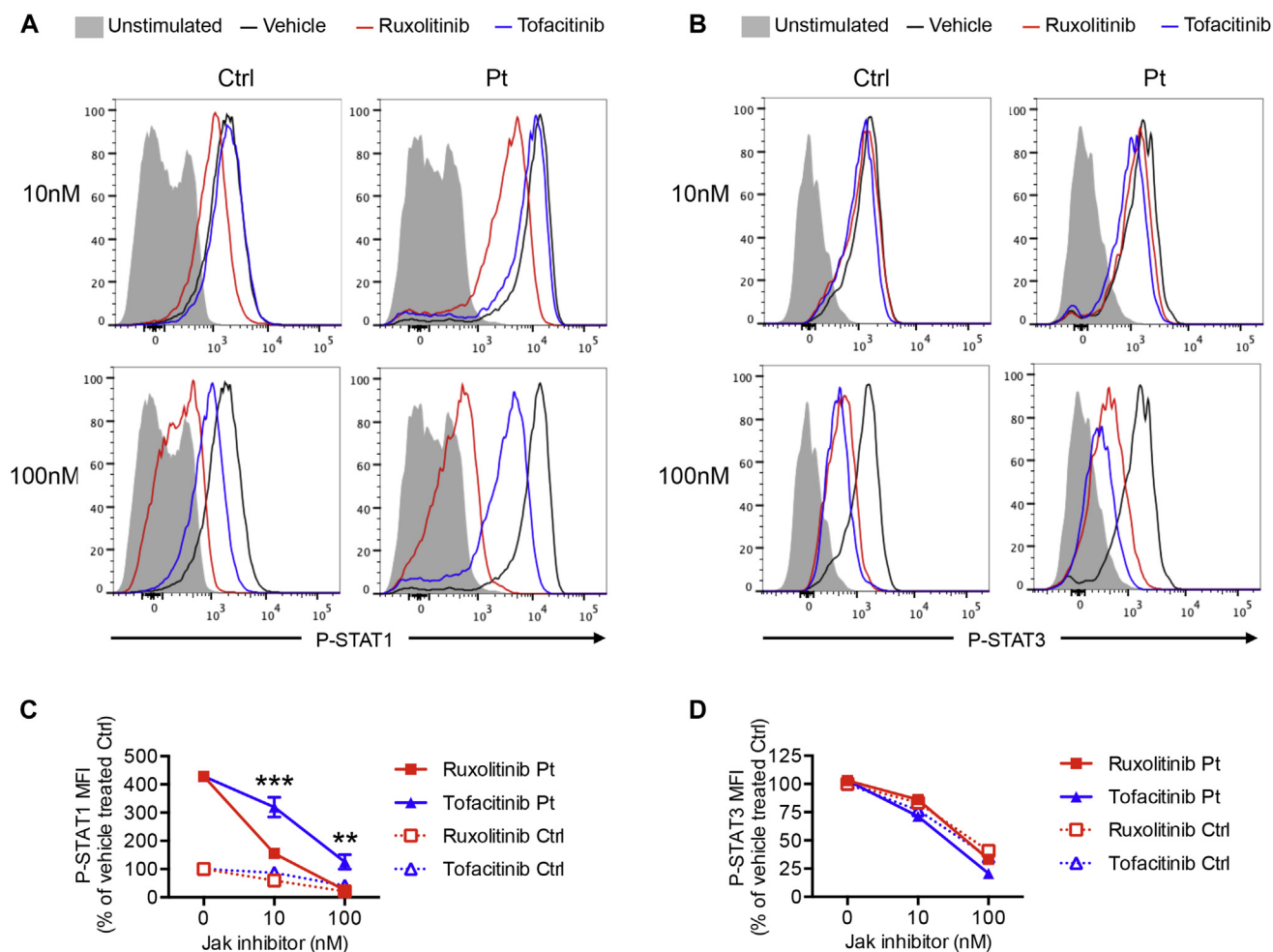
FIG 4. Different JAK inhibitors variably inhibit STAT1 and STAT3 phosphorylation *in vitro*. **A,** Phospho-STAT1 *(P-STAT1)* expression on IFN-β stimulation in CD4$^+$ T cells from a control subject and the *STAT1^{E545K}* patient treated *in vitro* with 10 and 100 nmol/L concentrations of ruxolitinib *(red curve)* and tofacitinib *(blue curve)* or vehicle (dimethyl sulfoxide, *black curve*). Plain gray corresponds to unstimulated cells. **B,** Phospho-STAT1 mean fluorescence intensity *(MFI)* expressed as percentage of maximum vehicle-treated control CD4$^+$ T cells shown in Fig 4, *A.* **C,** Phospho-STAT3 expression on IL-21 stimulation in CD4$^+$ T cells from a control subject and the *STAT1^{E545K}* patient treated *in vitro* with 10 and 100 nmol/L concentrations of ruxolitinib *(red curve)* and tofacitinib *(blue curve)* or vehicle. Plain gray corresponds to unstimulated cells. **D,** Phospho-STAT3 mean fluorescence intensity *(MFI)* expressed as a percentage of maximum vehicle-treated control CD4$^+$ T cells shown in Fig 4, *C.* **P < .001 and ***P < .0001, 2-way ANOVA with posttest analysis.

mutation, which is known to confer GOF activity based on previous reports in the literature.[13,26,27] As expected, CD4$^+$ T cells from patient 2 displayed exaggerated STAT1-phosphorylation in response to *in vitro* stimulation with type I and II interferons, which could also be mitigated by *in vitro* treatment with ruxolitinib (see Fig E2 in this article's Online Repository at www.jacionline.org). Importantly, patient 2 had chronic mucocutaneous candidiasis and opportunistic infectious without any clinical evidence of autoimmunity and had an increase in the fraction of circulating CXCR5$^+$PD1$^+$ T$_{FH}$ cells (Fig 3, *C*). The T$_{FH}$ cells of both patient 1 and patient 2 exhibited high expression of the pro-T$_H$1 chemokine receptor CXCR3 and decreased expression of the pro-T$_H$17 chemokine receptor CCR6, which is in agreement with previous studies (Fig 3, *D*).[37,38]

The JAK1/2 inhibitor ruxolitinib suppresses dysregulated *STAT1^{E545K}* phosphorylation induced by interferons

The JAK inhibitors ruxolitinib and tofacitinib, which primarily target JAK1/2 and JAK3, respectively, have been used to target dysregulated JAK/STAT activity in patients with different clinical conditions.[10,24] To investigate which of these 2 JAK inhibitors is most specific in normalizing STAT1^{E545K} activity without interfering with STAT3 signaling relevant to T$_H$17 differentiation, we tested the effects of ruxolitinib and tofacitinib on STAT1 and STAT3 activation in response to IFN-β and IFN-γ or IL-21 stimulation, respectively. Both drugs suppressed STAT1 and STAT3 phosphorylation in CD4$^+$ T cells from patient 1 and control subjects in a concentration-dependent manner. Ruxolitinib was more selective in suppressing STAT1 phosphorylation in
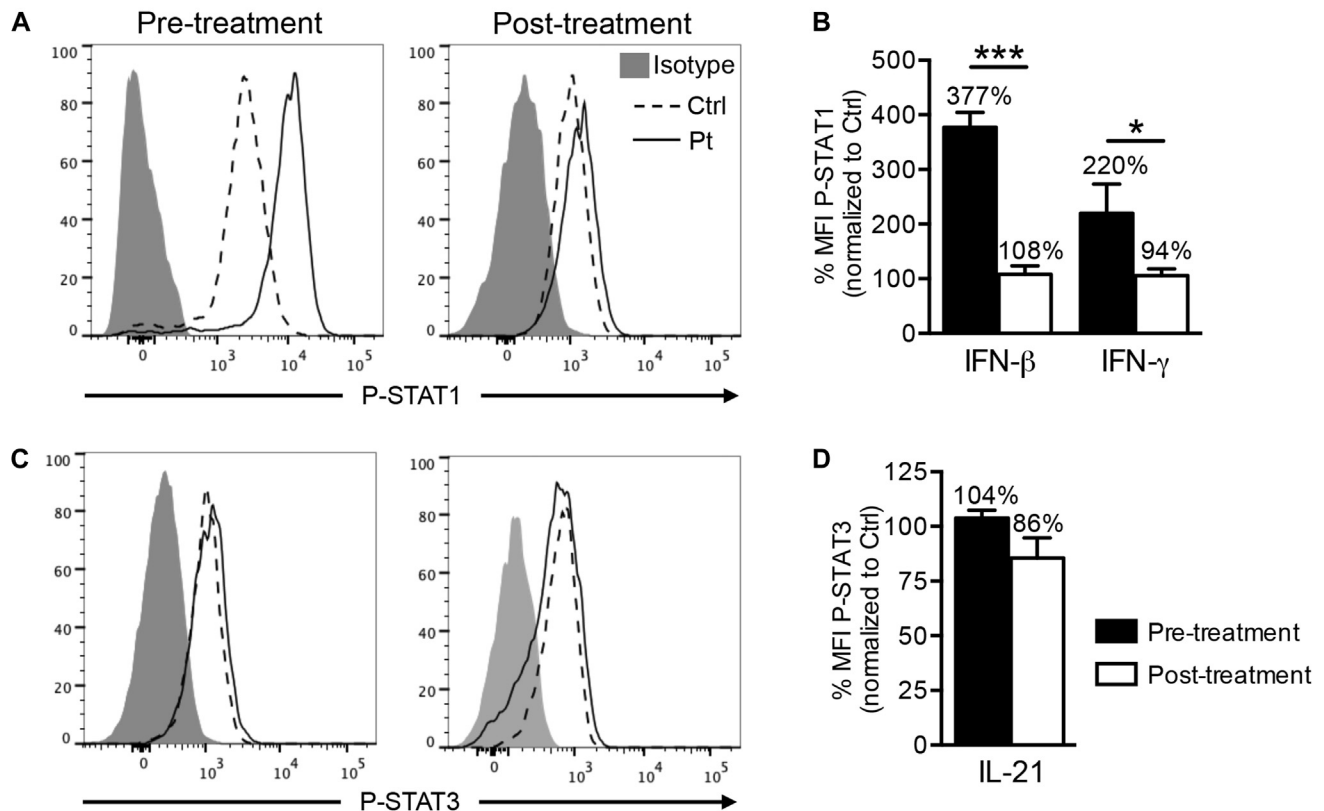
FIG 5. *In vivo* ruxolitinib treatment differentially controls STAT1 phosphorylation. **A,** Expression of phospho-STAT1 *(P-STAT1)* in CD4$^+$ T cells of the *STAT1^{E545K}* patient and control subject before and after *in vivo* therapy with ruxolitinib after IFN-β stimulation. **B,** Histogram represents phospho-STAT1 mean fluorescence intensity *(MFI)* normalized to expression in control CD4$^+$ T cells after IFN-β or IFN-γ stimulation before and after *in vivo* therapy with ruxolitinib. **C,** Expression of phospho-STAT3 in CD4$^+$ T cells of the *STAT1^{E545K}* patient and control subject before and after *in vivo* therapy with ruxolitinib after IL-21 stimulation. **D,** Histogram represents phospho-STAT3 MFI normalized to expression in control CD4$^+$ T cells after IL-21 stimulation before and after *in vivo* therapy with ruxolitinib. *$P < .05$ and ***$P < .001$.

response to IFN-β stimulation compared with tofacitinib, which is reflective of a lesser half-maximal inhibitory concentration (IC$_{50}$) necessary to block JAK1/2 activation (Fig 4, *A*).[39] In contrast, ruxolitinib was more sparing toward STAT3 phosphorylation in response to IL-21 stimulation, which is reflective of its higher IC$_{50}$ toward JAK3 compared with tofacitinib (Fig 4, *B*). Optimal effects were achieved with ruxolitinib at a concentration of 10 nmol/L, which decreased the STAT1 phosphorylation in the patient's CD4$^+$ T cells from more than 400% before treatment to approximately 150% of the STAT1 activity in vehicle-treated control CD4$^+$ T cells (Fig 4, *C*) while maintaining more than 80% of baseline STAT3 activity (Fig 4, *D*). The suppressive effect of tofacitinib on STAT1 and STAT3 phosphorylation in CD4$^+$ T cells from control subjects and the patient in response to IFN-β and IL-21 stimulation was dose dependent but nonselective with equal IC$_{50}$ values for STAT1 and STAT3, making it less suitable to treat isolated STAT1 hyperreactivity (Fig 4).

JAK inhibitor treatment controls STAT1 phosphorylation

Based on these *in vitro* data, we started treating the *STAT1^{E545K}* patient (patient 1) with ruxolitinib. We adjusted the ruxolitinib treatment dose in the patient so that STAT1 phosphorylation in response to stimulation with IFN-β and IFN-γ in the patient's CD4$^+$ T cells decreased to approximately 100% relative to that in control CD4$^+$ T cells (Fig 5, *A* and *B*). At this dose, which is equivalent to 10 mg/m^2 BSA per day, the patient's STAT3 phosphorylation in CD4$^+$ T cells in response to IL-21 stimulation was maintained at greater than 80% relative to that in control CD4$^+$ T cells, matching our *in vitro* findings (Fig 5, *C* and *D*).

Ruxolitinib treatment normalizes amplified T$_H$1 and improves impaired T$_H$17 responses

After 3 to 4 months of ruxolitinib therapy at the target dose, the IFN-γ production in circulating CD4$^+$ T cells from the patient decreased significantly, whereas IL-17 production in circulating CD4$^+$ T cells initially remained low despite clinical improvement in mucocutaneous candidiasis and diarrhea. After more than 1 year of therapy with ruxolitinib and after discontinuation of all other immunosuppressive medications, IFN-γ production in CD4$^+$ T cells from the *STAT1^{E545K}* patient remained suppressed to the level seen in normal control cells, whereas IL-17 production increased along with consolidation of the clinical picture (Fig 6, *A* and *B*). To assess whether ruxolitinib also has an effect on the aberrant priming of undifferentiated cells, we investigated the
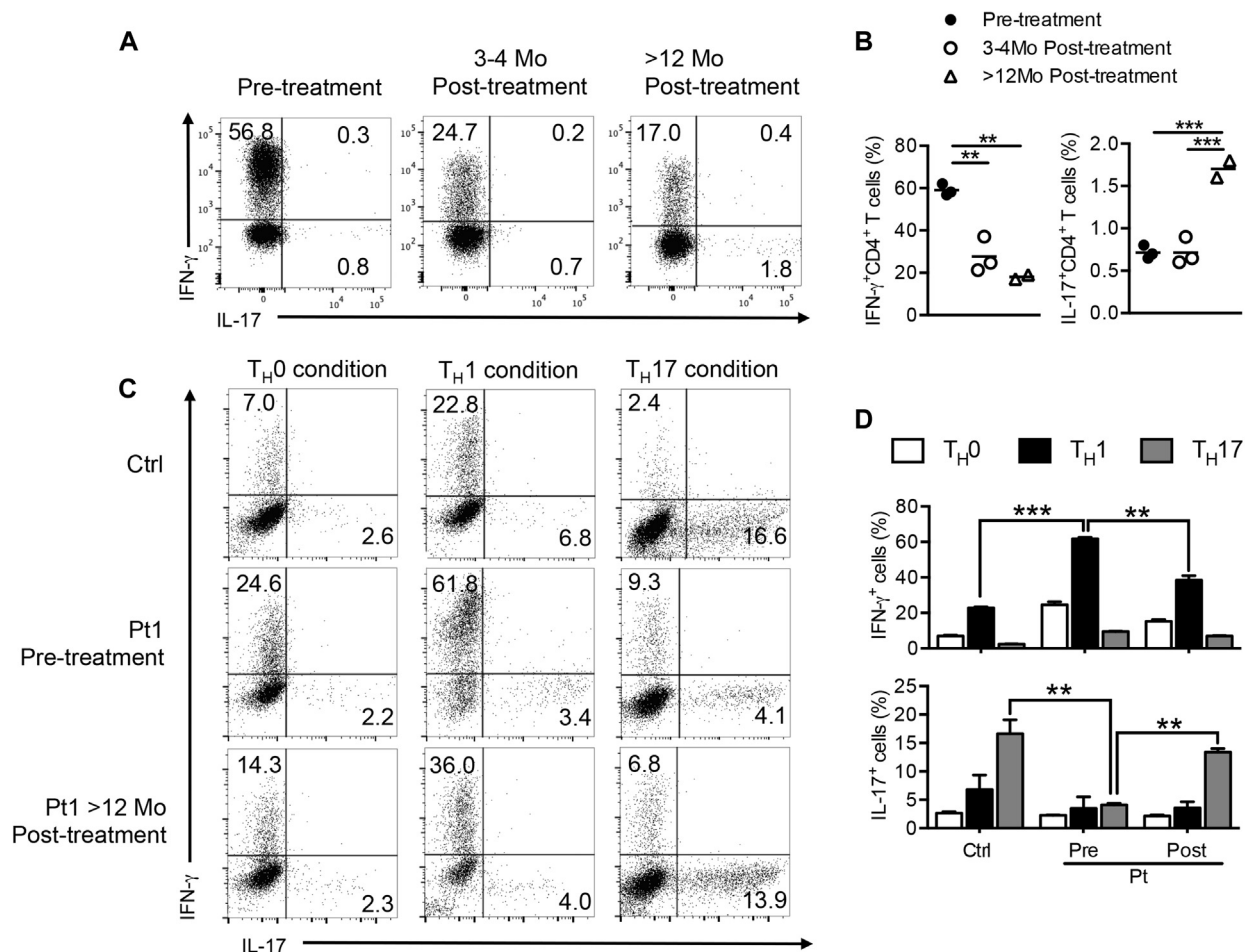
FIG 6. Ruxolitinib treatment normalizes amplified T_H1 and strengthens impaired T_H17 responses. **A,** Expression of IFN-$\gamma$ and IL-17 in CD4$^+$ T cells of patient 1 before and after *in vivo* therapy with ruxolitinib at target dose after 3 to 4 months and greater than 12 months, respectively. **B,** Histograms represent frequencies of IFN-γ– and IL-17–producing CD4$^+$ T cells shown in panel Fig 6, *A.* **P < .01 and ***P < .001, unpaired 2-tailed Student *t* test. **C,** Expression of IFN-γ and IL-17 in naive CD4$^+$ T cells from a control subject and the *STAT1^{E545K}* patient cultured under T_H0, T_H1, and T_H17 conditions before and after initiation of ruxolitinib treatment. **D,** Histograms represent frequency of IFN-γ– and IL-17–producing CD4$^+$ T cells under T_H0, T_H1, and T_H17 conditions, respectively. Pretreatment samples were obtained at least 6 months after ATG and rituximab treatment. Posttreatment samples were obtained after at least 12 months of ruxolitinib treatment at target dose. One representative experiment of 2 is shown. **P < .01 and ***P < .001, unpaired 2-tailed Student *t* test (Fig 6, *B*) or 2-way ANOVA (Fig 6, *D*) with posttest analysis.

capacity of naive CD4$^+$ T cells from patient 1 to polarize into IFN-γ– or IL-17–producing T_H1 or T_H17 cells, respectively, by means of *in vitro* differentiation under T_H0 (anti-CD2/CD3/28), T_H1 (anti-CD2/CD3/28 and IL-12), and T_H17 (anti-CD2/CD3/28, IL-6, IL-23, and TGF-β1) conditions (Fig 6, *C* and *D*). Our results revealed that the patient's naive CD4$^+$ T cells were biased to adopt a T_H1 fate with marked skewing toward IFN-γ production under all 3 conditions compared with control T cells. In contrast, IL-17 production was suppressed, especially under T_H17-polarizing conditions. Importantly, the priming of the *STAT1^{E545K}* mutation toward a T_H1/T_C1 phenotype and antagonizing T_H17 differentiation was almost entirely reversible with long-term treatment (>12 months) of the patient with ruxolitinib. No further drug was added to the *in vitro* culture conditions.

Ruxolitinib maintenance therapy reverses dysregulated T_{FH} cell expansion associated with the *STAT1^{E545K}* mutation

To investigate whether ruxolitinib is also effective in controlling the augmented T_{FH} response and possible T_{FH} priming caused by *STAT1^{E545K}*, we assessed the *in vitro* differentiation capacity of naive CD4$^+$ T cells from patient 1 into T_{FH} cells with TGF-β1, IL-12, and IL-23 before treatment with ruxolitinib and at multiple time points after (3 months, 12 months, and thereafter).[40] After only 3 months of ruxolitinib at the target dose, numbers of circulating T_{FH} cells in the *STAT1^{E545K}* patient normalized down to control levels (Fig 7, *A* and *B*) and remained stable over 12 months thereafter (data not shown).

To generate evidence that the enlarged T_{FH} compartment is a primary phenotype of the *STAT1^{E545K}* mutation and not a
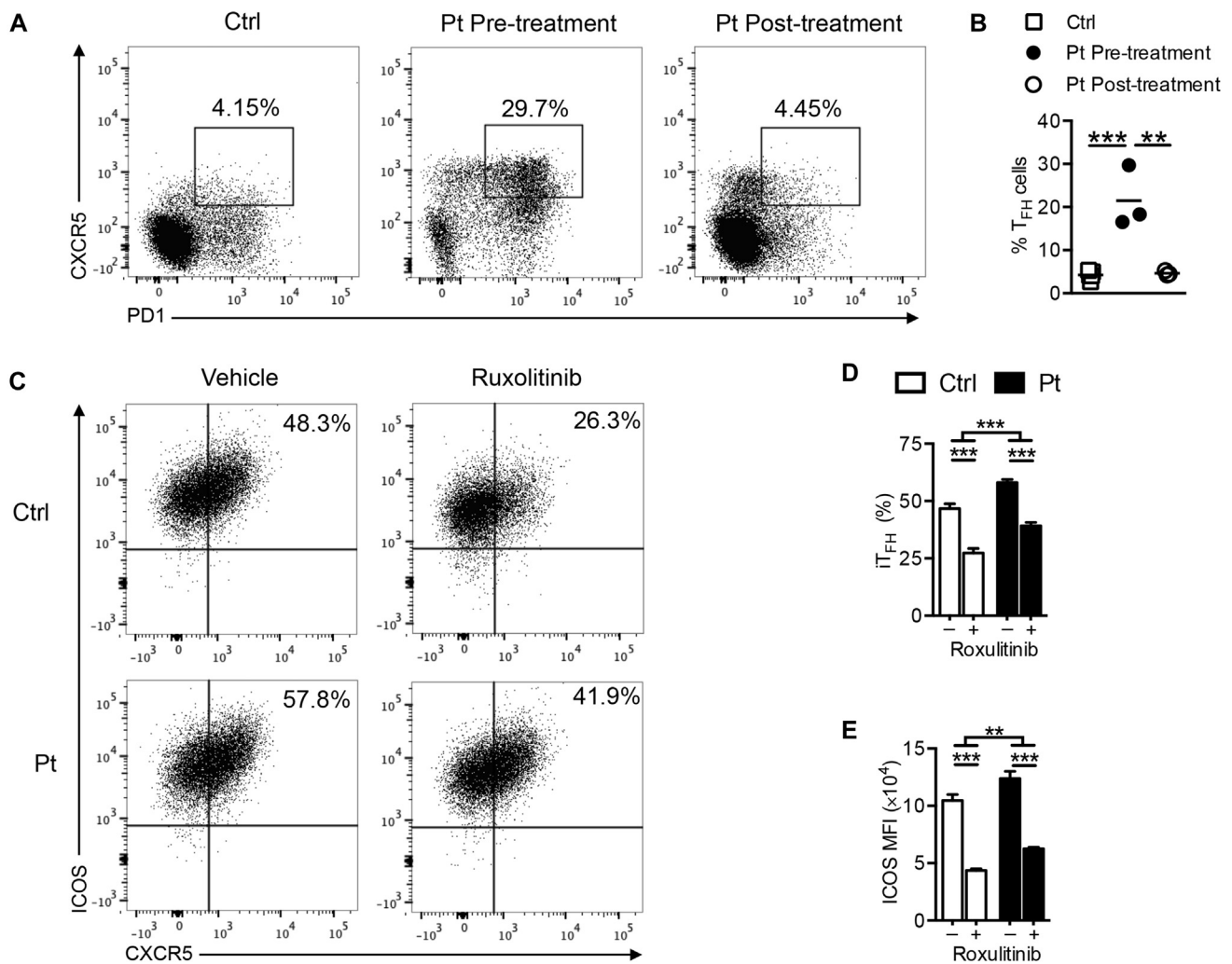
FIG 7. Ruxolitinib treatment corrects the exacerbated T_{FH} response in the $STAT1^{E545K}$ patient. **A,** CXCR5 and PD1 expression in CD4$^+$ T cells in the $STAT1^{E545K}$ patient before and after treatment with ruxolitinib at target dose for 3 months compared with control subjects. **B,** Histograms represent frequencies of T_{FH} cells in the $STAT1^{E545K}$ patient before and after treatment compared with control subjects. **C,** CXCR5 and ICOS expression in *in vitro*–differentiated T_{FH}-like cells from the patient and control subjects stimulated with TGF-β1, IL-12, and IL-23 in the presence or absence of ruxolitinib. **D,** Histograms represent frequencies of *in vitro*–differentiated T_{FH} cells with and without ruxolitinib in the patient and control subjects. **E,** ICOS mean fluorescence intensity *(MFI)* in *in vitro*–differentiated T_{FH} cells with and without ruxolitinib in the patient and control subjects. **P < .01 and ***P < .001, 1-way (Fig 7, *B, D,* and *E*) and 2-way (Fig 7, *D* and *E*) ANOVA with posttest analysis.

consequence of the longstanding history of autoimmune disease in our patient, we performed *in vitro* polarization studies showing that naive CD4$^+$ T cells from patient 1 had a profoundly exaggerated response to stimulation with TGF-β1, IL-12, and IL-23 compared with control cells, which led to the development of an expanded population of CXCR5$^+$ICOS$^+$ T_{FH}-like cells with higher ICOS expression levels. Ruxolitinib inhibited *in vitro* T_{FH} cell development in response to TGF-β1, IL-12, and IL-23, leading to a number of CXCR5$^+$ICOS$^+$ T_{FH}-like cells in the patient with the $STAT1^{E545K}$ mutation that was comparable with that in control subjects before treatment (Fig 7, *C-E*).

DISCUSSION

In this report we describe that a patient with a novel $STAT1^{E545K}$ GOF mutation in the linker domain, which is

associated with increased STAT1 phosphorylation, immune dysregulation, and intractable life-threatening autoimmune cytopenias, favorably responded to therapy with ruxolitinib. Long-term therapy addressed all immunophenotypic features of the disease, including cytokine-induced STAT1 hyperphosphorylation, amplified T_H1 and T_{FH} cell differentiation, impaired T_H17 immunity, and the respective aberrant priming of naive cells. Ruxolitinib controlled the autoimmune cytopenias, cured mucocutaneous candidiasis and diarrhea, led to a gradual amelioration of pulmonary function (forced vital capacity was 90% and FEV_1 was 80% after ruxolitinib treatmeant, compared with a forced vital capacity of 75% and FEV_1 of 66% prior to initiation of therapy), and allowed us to wean the patient off all other immunosuppressive therapy. Initial concerns that ruxolitinib could cause JAK2-mediated dose-limiting myelosuppression and anemia proved unsubstantiated. Thus JAK inhibitor therapy represents a rational

and effective therapy in patients with this disease. As with all immunomodulatory and immunosuppressive medications, careful clinical surveillance for side effects, including serious infections and malignancy, is warranted.

Like other *STAT1* GOF mutations, the *STAT1^E545K* mutation augmented STAT1 phosphorylation in response to cytokine signaling. However, unlike other common *STAT1* GOF mutations, it potentiated STAT1 phosphorylation without affecting dephosphorylation after withdrawal of the activating cytokine.[14] Also, it did not perturb the basal levels of phospho-STAT1 absent cytokine stimulation, suggesting that it promoted increased recruitment of STAT1 at the respective cytokine receptor. Of note, STAT3 phosphorylation was normal.

The *STAT1^E545K* mutation augmented the *in vitro* polarization of naive CD4$^+$ T cells into T$_H$1 and T$_{FH}$ cell subsets while rendering them resistant to T$_H$17 polarization. Similar skewing of helper T cell subsets was also observed *in vivo*, with the patient showing increased T$_H$1 and T$_{FH}$ but decreased T$_H$17 cell counts in the circulation. Suppressed T$_H$17 differentiation was noted despite normal STAT3 phosphorylation. Our findings are consistent with those of recent studies demonstrating that *STAT1* GOF mutations act distally to suppress STAT3 activation of components of the T$_H$17 transcriptional program, including *RORC*, without affecting cytokine-mediated STAT3 phosphorylation.[41] Surprisingly, the *STAT1^E545K* mutation was associated with a markedly expanded pool of circulating T$_{FH}$ cells. Similar observations were made in a patient (patient 2) with a different *STAT1* GOF mutation affecting the DNA-binding domain who was clinically free from any signs of autoimmunity. These findings suggest that a dysregulated T$_{FH}$ cell response is a primary feature of increased STAT1 activity independent of and not secondary to clinical autoimmunity. The molecular mechanisms leading to this enlarged T$_{FH}$ cell compartment are not clear. T$_{FH}$ cell expansion has been associated with humoral autoimmunity, and several monogenic immune dysregulatory diseases with humoral autoimmunity are associated with an expanded T$_{FH}$ cell pool, including cytotoxic T lymphocyte–associated antigen 4 and LPS-responsive beige-like anchor protein deficiency.[36,42]

By decreasing STAT1 hyperphosphorylation, JAK inhibitors combat the sequelae of unopposed interferon release, normalize T$_H$1 and T$_{FH}$ cell responses, and treat autoimmunity. In our studies long-term JAK inhibitor treatment also promoted T$_H$17 differentiation of naive CD4$^+$ T cells *in vitro* and rescued IL-17 production *in vivo*, which was clinically reflected by a significant improvement in mucosal immunity under ruxolitinib therapy. This is in line with the observations of Higgins et al[10] and Mössner et al[25] who reported improvement of oral candidiasis in response to ruxolitinib and relapse as the drug was withdrawn. Our concerns that JAK inhibition could compromise mucosal immunity further by decreasing STAT3 activity proved unsubstantiated because ruxolitinib only had a minor effect on STAT3 signaling.

The observation that ruxolitinib therapy reversed the exaggerated T$_{FH}$ phenotype and priming caused by *STAT1^E545K* in its entirety is concordant with its ability to control autoimmune manifestations in our patient over a period of more than 18 months. These observations suggest a role for JAK inhibitors as a maintenance treatment to prevent the development of further autoimmune disease, for which patients with *STAT1* GOF mutations are at extremely high risk over their lifetime. The availability of a targeted small-molecule therapy is particularly relevant in severely affected patients for whom a donor for

allogeneic hematopoietic stem cell transplantation is not available. Even with a suitable donor, the extent of autosensitization and allosensitization in patients with a longstanding history of autoimmunity together with their inherent underlying comorbidities often call the indication to proceed with an allogeneic hematopoietic stem cell transplantation into question.

The findings described above have implications for a broad patient population. Because *STAT1* GOF mutations can present with a wide range of clinical phenotypes, heightened clinical vigilance should prompt the physician to consider this diagnosis in any patient with autoimmune disease associated with mucocutaneous candidiasis or other opportunistic infections. Finally, this case illustrates how profoundly knowledge about the molecular underpinnings of autoimmune conditions can affect therapy and outcome.


Key messages

- A *STAT1^E545K* GOF mutation mediated T$_H$1/T$_C$1 skewing, T$_H$17 cell suppression, and an exaggerated T$_{FH}$ cell response.
- The JAK inhibitor ruxolitinib mitigated STAT1 hyperphosphorylation, normalized T$_H$1 and T$_{FH}$ cell differentiation, and improved T$_H$17 cell development both *in vitro* and *in vivo*.

REFERENCES

1. Boisson-Dupuis S, Kong XF, Okada S, Cypowyj S, Puel A, Abel L, et al. Inborn errors of human STAT1: allelic heterogeneity governs the diversity of immunological and infectious phenotypes. Curr Opin Immunol 2012;24:364-78.
2. Subramaniam PS, Torres BA, Johnson HM. So many ligands, so few transcription factors: a new paradigm for signaling through the STAT transcription factors. Cytokine 2001;15:175-87.
3. O'Shea JJ, Holland SM, Staudt LM. JAKs and STATs in immunity, immunodeficiency, and cancer. N Engl J Med 2013;368:161-70.
4. van de Veerdonk FL, Plantinga TS, Hoischen A, Smeekens SP, Joosten LA, Gilissen C, et al. STAT1 mutations in autosomal dominant chronic mucocutaneous candidiasis. N Engl J Med 2011;365:54-61.
5. Hori T, Ohnishi H, Teramoto T, Tsubouchi K, Naiki T, Hirose Y, et al. Autosomal-dominant chronic mucocutaneous candidiasis with STAT1-mutation can be complicated with chronic active hepatitis and hypothyroidism. J Clin Immunol 2012;32:1213-20.
6. Liu L, Okada S, Kong XF, Kreins AY, Cypowyj S, Abhyankar A, et al. Gain-of-function human STAT1 mutations impair IL-17 immunity and underlie chronic mucocutaneous candidiasis. J Exp Med 2011;208:1635-48.
7. Nahum A. Dala II. Clinical manifestations associated with novel mutations in the coiled-coil domain of STAT1. LymphoSign J 2014;1:97-103.
8. Roifman C. Monoallelic STAT1 mutations and disease patterns. LymphoSign J 2014;1:57-9.
9. Sharfe N, Nahum A, Newell A, Dadi H, Ngan B, Pereira SL, et al. Fatal combined immunodeficiency associated with heterozygous mutation in STAT1. J Allergy Clin Immunol 2014;133:807-17.
10. Higgins E, Al Shehri T, McAleer MA, Conlon N, Feighery C, Lilic D, et al. Use of ruxolitinib to successfully treat chronic mucocutaneous candidiasis caused by gain-of-function signal transducer and activator of transcription 1 (STAT1) mutation. J Allergy Clin Immunol 2015;135:551-3.e3.
11. Yamazaki Y, Yamada M, Kawai T, Morio T, Onodera M, Ueki M, et al. Two novel gain-of-function mutations of STAT1 responsible for chronic mucocutaneous candidiasis disease: impaired production of IL-17A and IL-22, and the presence of anti-IL-17F autoantibody. J Immunol 2014;193:4880-7.
12. Sampaio EP, Hsu AP, Pechacek J, Bax HI, Dias DL, Paulson ML, et al. Signal transducer and activator of transcription 1 (STAT1) gain-of-function mutations and disseminated coccidioidomycosis and histoplasmosis. J Allergy Clin Immunol 2013;131:1624-34.
13. Frans G, Moens L, Schaballie H, Van Eyck L, Borgers H, Wuyts M, et al. Gain-of-function mutations in signal transducer and activator of transcription 1 (STAT1):

chronic mucocutaneous candidiasis accompanied by enamel defects and delayed dental shedding. J Allergy Clin Immunol 2014;134:1209-13.e6.

14. Mizoguchi Y, Tsumura M, Okada S, Hirata O, Minegishi S, Imai K, et al. Simple diagnosis of STAT1 gain-of-function alleles in patients with chronic mucocutaneous candidiasis. J Leukoc Biol 2014;95:667-76.

15. Bohmer FD, Friedrich K. Protein tyrosine phosphatases as wardens of STAT signaling. JAKSTAT 2014;3:e28087.

16. Kumar N, Hanks ME, Chandrasekaran P, Davis BC, Hsu AP, Van Wagoner NJ, et al. Gain-of-function signal transducer and activator of transcription 1 (STAT1) mutation-related primary immunodeficiency is associated with disseminated mucormycosis. J Allergy Clin Immunol 2014;134:236-9.

17. Tóth B, Méhes L, Taskó S, Szalai Z, Tulassay Z, Cypowyj S, et al. Herpes in STAT1 gain-of-function mutation. Lancet 2012;379:2500.

18. Puel A, Cypowyj S, Marodi L, Abel L, Picard C, Casanova JL. Inborn errors of human IL-17 immunity underlie chronic mucocutaneous candidiasis. Curr Opin Allergy Clin Immunol 2012;12:616-22.

19. Romberg N, Morbach H, Lawrence MG, Kim S, Kang I, Holland SM, et al. Gain-of-function STAT1 mutations are associated with PD-L1 overexpression and a defect in B-cell survival. J Allergy Clin Immunol 2013;131:1691-3.

20. O'Shea JJ, Schwartz DM, Villarino AV, Gadina M, McInnes IB, Laurence A. The JAK-STAT Pathway: Impact on Human Disease and Therapeutic Intervention. Annu Rev Med 2015;66:311-28.

21. Aldave JC, Cachay E, Nunez L, Chunga A, Murillo S, Cypowyj S, et al. A 1-year-old girl with a gain-of-function STAT1 mutation treated with hematopoietic stem cell transplantation. J Clin Immunol 2013;33:1273-5.

22. Wildbaum G, Shahar E, Katz R, Karin N, Etzioni A, Pollack S. Continuous G-CSF therapy for isolated chronic mucocutaneous candidiasis: complete clinical remission with restoration of IL-17 secretion. J Allergy Clin Immunol 2013;132:761-4.

23. Faitelson Y, Bates A, Shroff M, Grunebaum E, Roifman CM, Naqvi A. A mutation in the STAT1 DNA-binding domain associated with hemophagocytic lymphohistiocytosis. LymphoSign J 2014;1:87-95.

24. Liu Y, Jesus AA, Marrero B, Yang D, Ramsey SE, Montealegre Sanchez GA, et al. Activated STING in a vascular and pulmonary syndrome. N Engl J Med 2014;371:507-18.

25. Mössner R, Diering N, Bader O, Forkel S, Overbeck T, Gross U, et al. Ruxolitinib induces interleukin 17 and ameliorates chronic mucocutaneous candidiasis caused by STAT1 gain-of-function mutation. Clin Infect Dis 2016;62:951-3.

26. Takezaki S, Yamada M, Kato M, Park MJ, Maruyama K, Yamazaki Y, et al. Chronic mucocutaneous candidiasis caused by a gain-of-function mutation in the STAT1 DNA-binding domain. J Immunol 2012;189:1521-6.

27. Soltesz B, Toth B, Shabashova B, Bondarenko A, Okada S, Cypowyj S, et al. New and recurrent gain-of-function STAT1 mutations in patients with chronic mucocutaneous candidiasis. J Med Genet 2013;50:567-78.

28. Ng PC, Henikoff S. Accounting for human polymorphisms predicted to affect protein function. Genome Res 2002;12:436-46.

29. Adzhubei IA, Schmidt S, Peshkin L, Ramensky VE, Gerasimova A, Bork P, et al. A method and server for predicting damaging missense mutations. Nat Methods 2010;7:248-9.

30. Emsley P, Cowtan K. Coot: model-building tools for molecular graphics. Acta Crystallogr D Biol Crystallogr 2004;60:2126-32.

31. Chen X, Vinkemeier U, Zhao Y, Jeruzalmi D, Darnell JE Jr, Kuriyan J. Crystal structure of a tyrosine phosphorylated STAT-1 dimer bound to DNA. Cell 1998;93:827-39.

32. Mao X, Ren Z, Parker GN, Sondermann H, Pastorello MA, Wang W, et al. Structural bases of unphosphorylated STAT1 association and receptor binding. Mol Cell 2005;17:761-71.

33. Biasini M, Bienert S, Waterhouse A, Arnold K, Studer G, Schmidt T, et al. SWISS-MODEL: modelling protein tertiary and quaternary structure using evolutionary information. Nucleic Acids Res 2014;42:W252-8.

34. Delano WL. The PyMol molecular graphics system. Palo Alto (Calif): DeLano Scientific; 2002.

35. Schmitt N, Liu Y, Bentebibel SE, Munagala I, Bourdery L, Venuprasad K, et al. The cytokine TGF-beta co-opts signaling via STAT3-STAT4 to promote the differentiation of human TFH cells. Nat Immunol 2014;15:856-65.

36. Charbonnier LM, Janssen E, Chou J, Ohsumi TK, Keles S, Hsu JT, et al. Regulatory T-cell deficiency and immune dysregulation, polyendocrinopathy, enteropathy, X-linked-like disorder caused by loss-of-function mutations in LRBA. J Allergy Clin Immunol 2015;135:217-27.

37. Ma CS, Wong N, Rao G, Avery DT, Torpy J, Hambridge T, et al. Monogenic mutations differentially affect the quantity and quality of T follicular helper cells in patients with human primary immunodeficiencies. J Allergy Clin Immunol 2015;136:993-1006.e1.

38. Ma CS, Wong N, Rao G, Nguyen A, Avery DT, Payne K, et al. Unique and shared signaling pathways cooperate to regulate the differentiation of human CD4+ T cells into distinct effector subsets. J Exp Med 2016;213:1589-608.

39. Quintas-Cardama A, Kantarjian H, Cortes J, Verstovsek S. Janus kinase inhibitors for the treatment of myeloproliferative neoplasias and beyond. Nat Rev Drug Discov 2011;10:127-40.

40. Kinnunen T, Chamberlain N, Morbach H, Choi J, Kim S, Craft J, et al. Accumulation of peripheral autoreactive B cells in the absence of functional human regulatory T cells. Blood 2013;121:1595-603.

41. Zheng J, van de Veerdonk FL, Crossland KL, Smeekens SP, Chan CM, Al Shehri T, et al. Gain-of-function STAT1 mutations impair STAT3 activity in patients with chronic mucocutaneous candidiasis (CMC). Eur J Immunol 2015;45:2834-46.

42. Kuehn HS, Ouyang W, Lo B, Deenick EK, Niemela JE, Avery DT, et al. Immune dysregulation in human subjects with heterozygous germline mutations in CTLA4. Science 2014;345:1623-7.
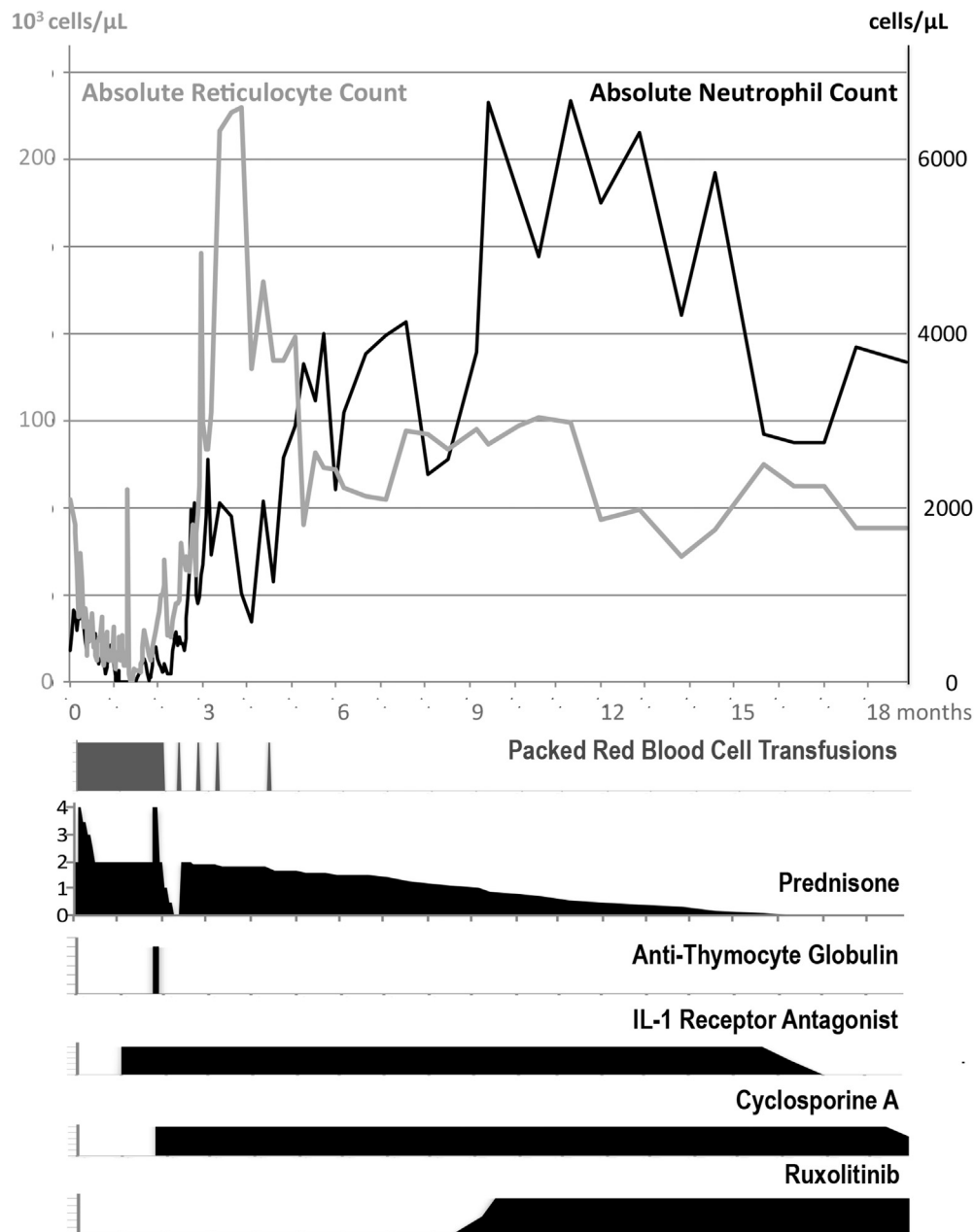
FIG E1. Hemoglobin and platelet count in response to pharmacotherapy. Graph depicts absolute reticulocyte count in 10^3 cells per microliter *(gray curve)* and absolute neutrophil count in cells per microliter *(black curve)* in response to changes in steroid dose, as well as therapy with ATG, the IL-1 receptor antagonist anakinra, cyclosporine, and ruxolitinib. Timing of packed red blood cell transfusions is indicated in dark gray. The prednisone dose is expressed in milligrams per kilogram body weight.
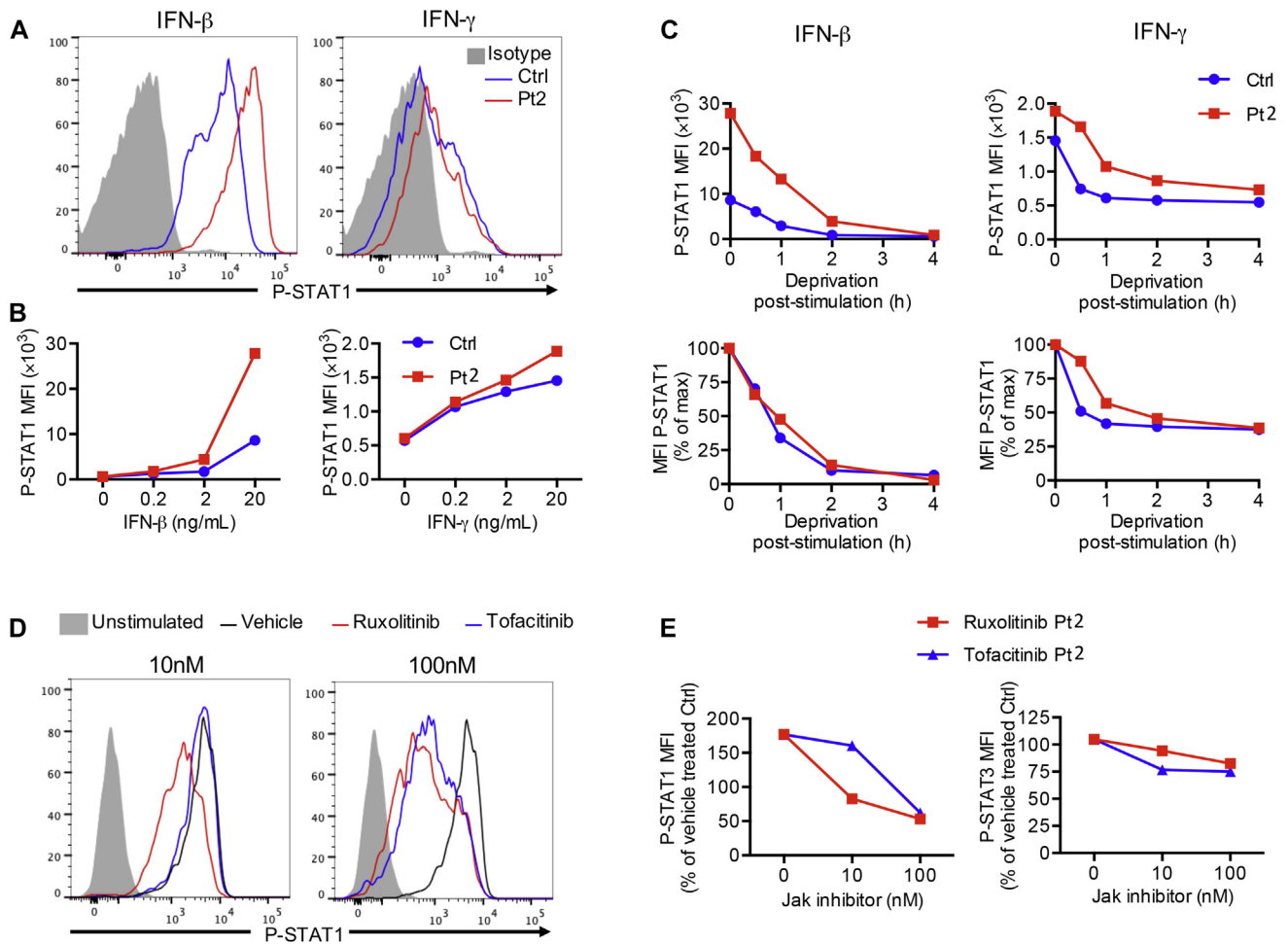
FIG E2. $STAT1^{T385M}$ mutation in patient 2 leads to hyperphosphorylation GOF. **A,** Phospho-STAT1 (P-STAT1) expression in CD4$^+$ T cells stimulated with IFN-β and IFN-γ in the $STAT1^{T385M}$ patient (patient 2) and control subjects. **B,** Dose-response curve of STAT1 phosphorylation induced with IFN-β and IFN-γ in CD4$^+$ T cells of patient 2 and control subjects. **C,** Dephosphorylation kinetics of phospho-STAT1 in response to deprivation of IFN-β and IFN-γ in CD4$^+$ T cells represented as absolute mean fluorescence intensity (*MFI*; *top*) and normalized to maximum expression before deprivation *(bottom)*. **D,** Phospho-STAT1 expression on IFN-β stimulation in CD4$^+$ T cells of patient 2 and control subject treated *in vitro* with ruxolitinib *(red curve)* and tofacitinib *(blue curve)* or vehicle (dimethyl sulfoxide, *black curve*). Plain gray corresponds to unstimulated cells. **E,** Phospho-STAT1 and phospho-STAT3 MFI expressed as percentage of maximum vehicle-treated control CD4$^+$ T cells shown in Fig E2, *D,* in response to increasing concentrations of ruxolitinib *(red curve)* and tofacitinib *(blue curve)*.